Journal of Geodynamics 51 (2011) 205–218

Contents lists available at ScienceDirect

Journal of Geodynamics

journal homepage: http://www.elsevier.com/locate/jog

Earthquake deformation in the northwestern Sierras Pampeanas of Argentina based on seismic waveform modelling

Patricia Alvarado[a,b,*], Victor A. Ramos[a,c]

[a] Consejo Nacional de Investigaciones Científicas y Técnicas (CONICET), Argentina
[b] Departamento de Geofísica y Astronomía, Facultad de Ciencias Exactas, Físicas y Naturales, Universidad Nacional de San Juan, Meglioli 1160 S, (5406) Rivadavia, San Juan, Argentina
[c] Laboratorio de Tectónica Andina, Facultad de Ciencias Exactas y Naturales, Universidad de Buenos Aires, Ciudad Universitaria, Pabellón II, Buenos Aires, Argentina

ARTICLE INFO

Article history:
Received 25 January 2010
Received in revised form 9 August 2010
Accepted 14 August 2010

Keywords:
Crustal earthquakes
Sierras Pampeanas
Andean foreland
Neotectonics
Seismic hazard

ABSTRACT

We investigate the seismic properties of modern crustal seismicity in the northwestern Sierras Pampeanas of the Andean retroarc region of Argentina. We modelled the complete regional seismic broadband waveforms of two crustal earthquakes that occurred in the Sierra de Velasco on 28 May 2002 and in the Sierra de Ambato on 7 September 2004. For each earthquake we obtained the seismic moment tensor inversion (SMTI) and tested for its focal depth. Our results indicate mainly thrust focal mechanism solutions of magnitudes M_w 5.8 and 6.2 and focal depths of 10 and 8 km, respectively. These results represent the larger seismicity and shallower focal depths in the last 100 years in this region. The SMTI 2002 and 2004 solutions are consistent with previous determinations for crustal seismicity in this region that also used seismic waveform modelling. Taken together, the results for crustal seismicity of magnitudes ≥5.0 in the last 30 years are consistent with an average *P*-axis horizontally oriented by an azimuth of 125° and *T*-axis orientation of azimuth 241° and plunge 58°. This modern crustal seismicity and the historical earthquakes are associated with two active reverse faulting systems of opposite vergences bounding the eastern margin of the Sierra de Velasco in the south and the southwestern margin of the Sierra de Ambato in the north. Strain recorded by focal mechanisms of the larger seismicity is very consistent over this region and is in good agreement with neotectonic activity during the last 11,000 years by Costa (2008) and Casa et al. (in press); this shows that the dominant deformation in this part of the Sierras Pampeanas is mainly controlled by contraction. Seismic deformation related to propagation of thrusts and long-lived shear zones of this area permit to disregard previous proposals, which suggested an extensional or sinistral regime for the geomorphic evolution since Pleistocene.

1. Introduction

The Andean foreland in Argentina is very seismically active at both slab and crustal depths (Barazangi and Isacks, 1976; Cahill and Isacks, 1992; Smalley et al., 1993; Gutscher et al., 2000; Pardo et al., 2002; Alvarado et al., 2009a). However the most significant examples of damaging earthquakes (1861, 1894, 1944, 1977 and 1985) are the events in the crust (depth < 35 km) of the Andean retroarc over the flat-slab subduction segment at about 31°S (Kadinsky-Cade, 1985; Langer and Bollinger, 1988; Langer and Hartzell, 1996; Alvarado and Beck, 2006; INPRES, 2010). The study of the largest earthquakes in San Juan using teleseismic data has revealed predominantly reverse focal mechanisms but different crustal depths of their sources (Chinn and Isacks, 1983; Kadinsky-Cade, 1985; Langer and Hartzell, 1996; Alvarado and Beck, 2006). These events are associated with the shortening in the thick-skinned Sierras Pampeanas and their interaction with the frontal part of the thin-skinned Precordillera fold and thrust belt (Fig. 1).

The region immediately north of 31°S is also characterized by active thick-skinned basement-cored uplifts of the western Sierras Pampeanas (Figs. 1 and 2) but it is much less known in terms of seismic activity. Global seismic location and relocation analyses to investigate the morphology of the subducted Nazca plate have shown a more inclined position of the slab from hypocentral depths greater than 150 km in this region (Barazangi and Isacks, 1976; Cahill and Isacks, 1992; Pardo et al., 2002). The occurrence of two damaging earthquakes of moderate magnitude in 2002 and 2004 with location in the overriding continental crust showed that the earthquake potential from intraplate events cannot be ignored. The study of this modern seismicity provides an opportunity to

* Corresponding author at: Departamento de Geofísica y Astronomía, Facultad de Ciencias Exactas, Físicas y Naturales, Universidad Nacional de San Juan, Meglioli 1160 S, (5406) Rivadavia, San Juan, Argentina. Tel.: +54 264 4234129 x177; fax: +54 264 4234980.
E-mail addresses: alvarado@unsj.edu.ar (P. Alvarado), andes@gl.fcen.uba.ar (V.A. Ramos).

0264-3707/$ – see front matter © 2010 Elsevier Ltd. All rights reserved.
doi:10.1016/j.jog.2010.08.002

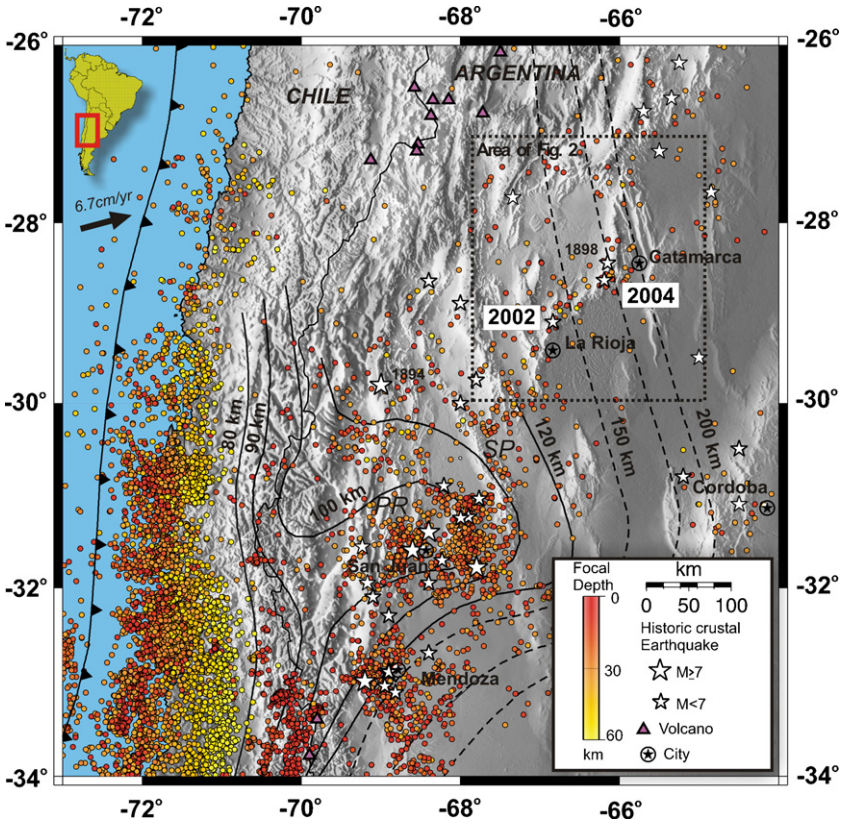

Fig. 1. Preliminary Determination Earthquakes – PDE of the National Earthquake Information Center – USGS (U.S.A.) and Instituto Nacional de Prevención Sísmica-INPRES (Argentina) seismic locations in the period 1998–2008. Stars show historical crustal seismicity from INPRES (2010) and the earthquakes in 2002 and 2004 here studied. Dashed-line contours represent the Wadati-Benioff zone by Cahill and Isacks (1992) and solid-line contours show depths to the subducted slab from Anderson et al. (2007). Note the greater size and frequency of crustal earthquake occurrence related to the interaction of the Precordillera (PR) and the Sierras Pampeanas (SP) over the flat-slab segment in comparison with the seismic activity of the region in the dotted-line box. Also shown is the Nazca-South America plate convergence velocity from GPS observations (Vigny et al., 2009) and active volcanoes (Kay et al., 1991).

learn more about the seismic deformation of this region, which may be more difficult using past earthquake history. According to CERESIS (2010) and INPRES (2010) only one event of probably similar earthquake size has occurred in the vicinity of the 2002 and 2004 epicenters more than 100 years ago (Fig. 1).

Seismic analyses using full regional broadband waveform modelling are definitely improving estimations of earthquake faulting geometry, depth and size of the larger seismicity in the Sierras Pampeanas. We present a characterization of the seismic sources of the 28 May 2002 and 7 September 2004 earthquakes using broadband regional seismic data. We have investigated the tectonic implications of these earthquake occurrences with epicenters in the Sierra de Velasco and Sierra de Ambato, respectively (Fig. 2). This study can help in identifying hazardous faults, predicting the nature and probability of earthquakes on those faults, and constraining the extent and magnitude of these events.

2. Seismotectonic setting

The Andean compression generates crustal earthquakes in the retroarc like the 2002 Velasco and the 2004 Ambato earthquakes, located more than 400 km to the east away from the oceanic trench. The global catalogue from the Preliminary Determination of Epicenters of the National Earthquake Information Center (PDE-NEIC) of the United States Geological Service (U.S.A.) has reported 140 earthquakes with magnitudes >4.0 and depths <50 km for the region between 27.5°S and 30°S and 65°W and 68°W between 1998 and 2008. However, only 46 events were felt locally according to reports from the local seismic network of the Instituto Nacional de Prevención Sísmica (INPRES) of Argentina in that period. The comparison of the seismic activity during 1900–1995 between the region where the Nazca plate is subducting horizontally (31°S–32°S) and the studied region located to the north, characterized by an increase in the angle of the subducted slab (Fig. 1), shows a decrease from south to north of 80% in the energy released by crustal seismicity reported with depths <70 km (Gutscher et al., 2000; Gutscher, 2002). Although less frequent than in the flat-slab segment, the occurrence of the 1898, 2002 and 2004 earthquakes confirms that this region is capable of earthquakes of magnitude >6.0 with possible activation of hazardous faults (Araujo et al., 2005; Costa, 2008; INPRES, 2010; Fig. 2). Unfortunately a quantitative source characterization of the 1898 historical event is difficult to attempt because of the unavailability of seismic records from that time, but it is possible to study in more detail the 2002 and 2004 damaging earthquakes.

Small-to-moderate seismicity instrumentally recorded can provide valuable constraints to help understanding the active tectonics of a region. Our approach includes available estimations of source parameters from past studies which used seismic waveform modelling and the new constraints of the 2002 and 2004 earthquakes from this work which involve the seismic moment tensor inversion (SMTI) of broadband regional seismic data. Thus, Table 1 and Fig. 2 show previous determinations for three earthquakes that used the Nábělek's method (Nábělek, 1984) and teleseismic body wave modelling (Assumpção and Araujo, 1993). Also listed in Table 1 is the seismic moment tensor inversion solution of one event that occurred on 18 May 2001. This determination utilized regional broadband seismic data collected during the Chile–Argentina Geophysical Experiment (CHARGE) (Alvarado et al., 2005a). Another available information for two smaller-sized

Table 1
Crustal earthquakes in the region with source parameters constrained from waveform modelling. Parameters for each fault-plane solution follow the same convention used by Alvarado et al. (2005a). References: AA, Assumpção and Araujo, 1993; APM, Araujo et al., 2005; HVR, Harvard-CMT, online catalogue; AEA, Alvarado et al., 2005a.

Date (month/day/year)	Time (h:min:s)	Latitude (°)	Longitude (°)	Depth (km)	Magnitude	Seismic moment $M_0 \times 10^{17}$ (Nm)	Strike (°)	Dip (°)	Rake (°)	*P*-axis Az/plunge (°)	*T*-axis Az/plunge (°)	Reference
12/24/1979	00:13:40	−29.63	−66.87	27	M_b 5.4	0.41	168	65	41	290/07	28/46	AA
							58	53	148			
04/02/1983	05:58:36	−28.54	−66.59	38	M_b 5.5	0.35	208	30	87	120/15	307/75	AA
							31	60	92			
	05:58:40.8	−29.02	−66.13	40.1 ± 7.9	M_w 5.3	1.02	247	25	137	122/26	262/58	HVR
							17	73	71			
06/24/1989	12:58:39	−28.35	−66.3	22	M_b 5.4	3.3	53	42	89	324/03	156/87	AA
							234	48	91			
	12:58:47.1	−28.53	−66.2	21 (fixed)	M_w 5.5	2.04	88	77	−172	321/15	43/03	HVR
							357	82	−13			
06/13/2001	04:10:53	−27.69	−66.9	38.1 ± 8.8	M_w 5.0	0.418	209	30	70	134/17	346/71	HVR
							52	62	101			
12/15/2001	22:37:24	−29.337	−66.857	20 (20–40)	M_w 4.0	0.00966	14	41	82	290/04	162/84	AEA
							204	49	97			
05/28/2002	04:04:28	−29.15	−66.81	15 (fixed)	M_w 6.0	11.7	180	19	55	117/29	322/59	HVR
							36	74	101			
([a])	04:04:23	−29.106	−66.839	11	M_D 6.0		45	75	103	124/29	332.6/58	APM
							183	19.8	49.7			
	04:04:23	−29.11	−66.84	10	M_w 5.8	5.49	36	56	109	112/09	355/71	This study
							184	39	64			
09/07/2004	11:53:16	−28.91	−65.79	20 (fixed)	M_w 6.1	16.8	216	37	80	133/09	348/79	HVR
							48	54	97			
([a])	11:53:06	−28.6	−66.14	27	M_D 6.5		193	60	34	139/0.64	48/4	APM
							85	61	145			
	11:53:16	−28.73	−66.2	8	M_w 6.2	22.3	32	74	90	122/29	302/61	This study
							213	16	91			
03/14/2005	12:43:44.5	−28.86	−66.28	27.3 ± 1.0	M_w 5.1	0.506	247	54	136	126/01	217/54	HVR
							6	56	45			

[a] The focal mechanism solution is based only on P-wave first motions.

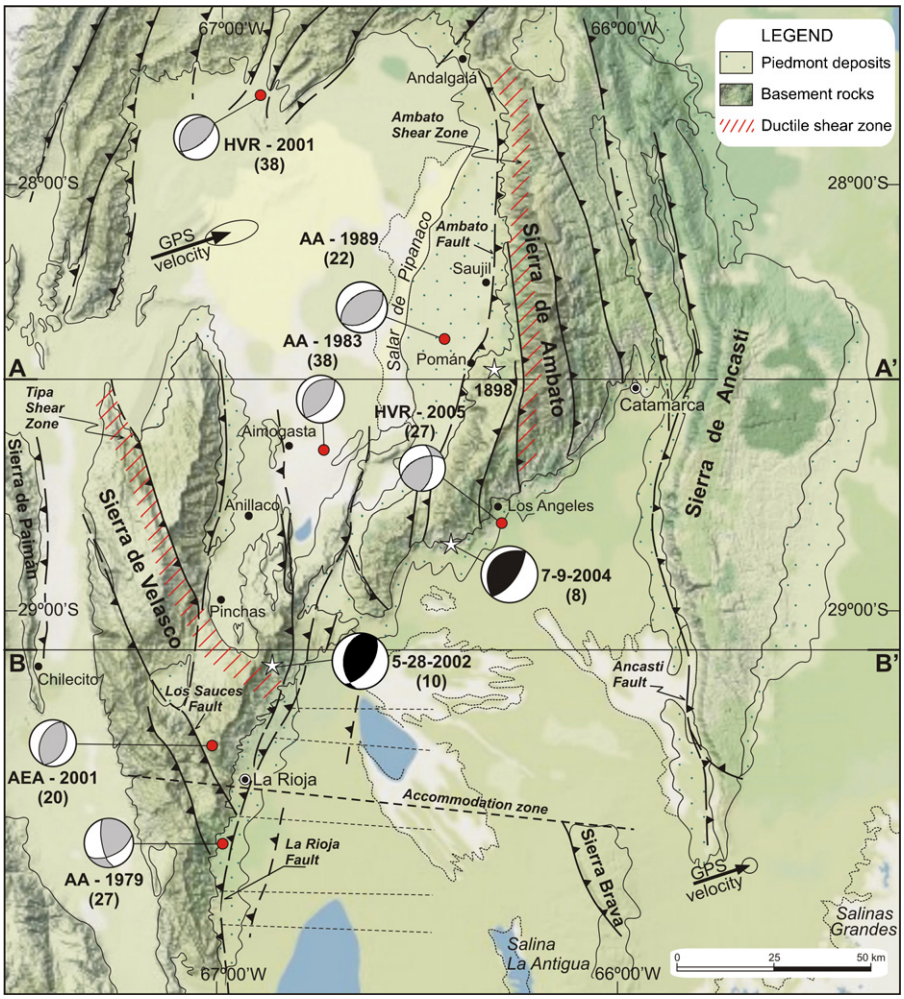

Fig. 2. Structure of Sierras Pampeanas in the study area with the main Andean basement thrusts (Ramos, 1999; Fisher et al., 2002; Costa, 2008). Focal mechanisms in lower hemisphere projection and source depths in parentheses from waveform modelling are shown for the larger crustal earthquakes (magnitudes between 4.0 and 6.2) (see Table 1 for references). Previous focal mechanism determinations are in gray compressional quadrants. Our constraints using the SMTI and regional broadband seismic data for the 2002 Velasco and the 2004 Ambato earthquakes are in black compressional quadrants. The historical earthquake in 1898 (INPRES, 2010) is also indicated. Also shown are GPS velocity vectors and their 95% confidence ellipses from Brooks et al. (2003). Location of a possible accommodation zone (long dashed lines) and seismic reflexion lines (short dashed lines) are after Fisher et al. (2002). Note the dominant reverse focal mechanisms. A–A′ and B–B′ are the locations of structural sections of Fig. 4.

earthquakes that occurred in the northern part of the studied region was obtained from the Harvard centroid moment tensor (Harvard CMT) catalogue (Fig. 2). We note that some earthquakes have more than one determination for the seismic source parameters. In this case we preferred constraints that used local and regional seismic waveform modelling instead of Harvard CMT solutions. The reason is that the CMT method uses long period (>40 s) teleseismic waveforms and consequently, it is more insensitive to the local seismic velocity structure. Thus, the CMT solution is a first order approximation to the seismic source parameters which also include the solution for the centroid seismic location (Dziewonski et al., 1981; Dziewonski and Woodhouse, 1983; Arvidsson and Ekström, 1998).

Most of the focal mechanisms in Table 1 indicate thrust fault plane solutions. They are consistent with the main N–S trending of the western Sierras Pampeanas ranges where the earthquakes are located. Fig. 2 shows two crustal levels of seismicity at depths of 8–10 km and 20–40 km. We note that there are some differences between crustal depth estimations for the same seismic events in the study region when using regional seismic data or teleseismic waveforms (e.g. Harvard CMT) (Fig. 3 and Table 1). In order to compare and contrast modelled crustal depth estimations, we have searched for more determinations in adjacent areas around the epicentral region of the 2002 and 2004 earthquakes. Thus we have

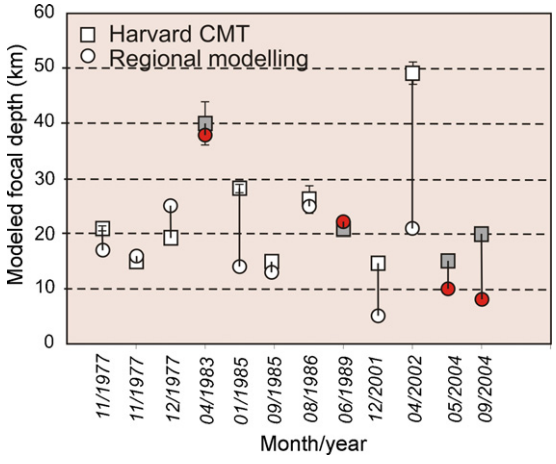

Fig. 3. Comparison between focal depths determined by Harvard CMT and other methods like Nabelek's and SMTI (see references in the text). Dark colors show the events in the study area (Fig. 2). White colors show other determinations in the Sierras Pampeanas outside of the epicentral area of the 2002 and 2004 earthquakes. Errors in depth constraints for CMT solutions are shown with bars. No error bars means fixed focal depths. Note that the CMT depths tend to be deeper than the focal depths obtained using other modelling methods, even for recent earthquakes.

selected earthquakes in the Sierras Pampeanas studied by Chinn and Isacks (1983), Kadinsky-Cade (1985), Triep (1979), Assumpção (1992) and Alvarado et al. (2005a) using depth-phase analysis and seismic data recorded by regional networks. The same earthquakes are large enough to have focal mechanism solutions in the Harvard CMT catalogue (Fig. 3). We note that most of the events have a fixed focal depth in their CMT solutions (Fig. 3). Overall most of the events studied using regional data modelling exhibit shallower focal depths that were not fixed in contrast to the CMT depths. These differences become larger for recent events that occurred after 2001 with discrepancies of up to ~30 km in their depth estimations. We believe that the smaller differences observed for the events that occurred before 1989 are due to the fact that their focal depths are based on depth phase determinations calculated by the International Seismological Centre-ISC which, were then used by the regional modelling or Harvard CMT method to initialize the corresponding iteration processing (Dziewonski et al., 1981). Thus the final focal depth result is around the initial (ISC) focal depth. By contrast, differences are larger when using methods that enable us to test each hypocenter depth independently during the waveform inversions. Better focal depths are obtained if more seismic regional station-components are used in the inversions and if different seismic velocity-structure models, more appropriate for representing raypaths travelling along the Andean structure and the eastern geologic terranes, are also taken into account (Alvarado et al., 2005a,b). This is the case for the earthquakes studied after 2001. Two examples are discussed in detail in the present work for the 2002 and 2004 crustal earthquakes.

Prediction of the present tectonic stress field has been attempted for several intraplate continental regions using numerical global modelling from multiple stress indicators involving focal mechanisms, well breakouts and drilling-induced fractures (e.g. Lithgow-Bertelloni and Guynn, 2004; World Stress Map WSM-Project, 2010). Some statistical analyses are available for other Andean foreland segments (Alvarado et al., 2005a; Guzmán et al., 2007; Guzmán and Cristallini, 2009). However, very little is known from direct observations for the region of study. We have used only eight focal mechanism determinations for the larger crustal seismicity in the area as a proxy to estimate average *P*- and *T*-axes, which strictly represent maximum shortening and maximum lengthening orientations bisecting the dilatational and compressional quadrants. We used a seismic moment tensor summation over these earthquakes (Table 1). These estimations represent the only source of data to constrain principal stress–strain orientations in this intraplate Andean foreland region (Heidbach et al., 2008).

Recent GPS surveys show one velocity vector of 8.2 ± 2.7 mm/year with orientation N76.5°E and acceptable values between N68.3°E and N79.5°E corresponding to a ~4-year period in the northwest part of the study region. Another GPS velocity vector of 3.4 ± 0.7 mm/year with trend of N75.4°E with acceptable values between N70.1°E and N77.7°E was observed over a 7.3-year period in the southeast part of the study region (Brooks et al., 2003) (Fig. 2). These observations clearly indicate a decrease from west to east in the magnitude of the GPS velocity vectors consistent with a shortening along a direction similar to the plate convergence orientation between the Nazca and South American plates (Kendrick et al., 2003; Vigny et al., 2009).

3. Geologic setting

Since the early proposal of González Bonorino (1950), the Sierras Pampeanas of central western Argentina were interpreted as basement-cored uplifts generated during the Andean deformation as a result of a compressive regime. This author proposed that listric reverse faults detached at lower crustal depths in brittle–ductile transitions are responsible for the basement structure; this is a hypothesis that was followed by most of the research conducted in the structure of the Sierras Pampeanas in later years (Jordan and Allmendinger, 1986; Introcaso et al., 1987; Ramos et al., 2002). One of the mechanisms linked to the uplift of the Sierras Pampeanas and the exposed thick-skinned style of deformation is the change from a steep to a shallower horizontal dip angle of the subducting Nazca plate that generated the Pampean flat-slab during the last 10 mys (Jordan et al., 1983a,b).

3.1. Description of the structure

Although the Sierra de Velasco and Sierra de Ambato ranges with elevations as high as 4500 m are bounded by reverse faults, they show a different tectonic style (Fig. 2). Overall, the Sierra de Ambato and its eastern region are dominated by west vergence reverse faults while the Sierra de Velasco and the southward region exhibit east vergence reverse faults (Ramos, 1999; Fisher et al., 2002; Ramos et al., 2002). This opposite vergence was explained by different mechanisms through time, mainly regarding to the intensive imbrications observed in the Ambato block east of the Sierra de Ambato (see Figs. 2 and 4).

The location of the epicenters of the recent moderate seismic activity matches two areas of important neotectonic features in the eastern margin of Sierra de Velasco and in the western margin of the Sierra de Ambato.

The eastern Sierra de Velasco area has a prominent north-trending neotectonic activity defined by fault scarps cutting Quaternary deposits and other geomorphic surfaces along the eastern piedmont La Rioja fault (Costa, 2008). This reverse fault is in the epicentral region of the 28 May 2002 earthquake. A series of minor synthetic secondary west-dipping faults were recognized at these latitudes at the subsurface in seismic lines by Fisher et al. (2002). In the surface, Quaternary deposits are affected by east verging thrusts providing evidences of an active uplift of the low relief hills north of La Rioja city. The La Rioja fault system north of the city has several splays, being the Anillaco branch the segment that accumulates most of the slip transfers, as inferred by the present topography (Fig. 2). The two small branches near Anillaco concentrate important neotectonic activity. Some other N–S trending-fault scarps have been observed to the west of La Rioja bounding the eastern flanks of the small ranges of the Sierra de Velasco (Fisher et al., 2002) and further south (Massabie et al., 1998).

Near La Rioja city there are two earthquakes (AA-1979 and AEA-2001) that show mainly thrust focal mechanisms consistent with the other source solutions (Fig. 2 and Table 1). Although their association with an individual fault is uncertain, the focal mechanisms can be interpreted as evidence of either motion along an NW-trending fault, or along an ENE-trending fault. Both deformation systems are present in the area. The NW-trending fault is coincident with the strike of Los Sauces Andean fault system described in the Quebrada de La Rioja, west of this city, by Aceñolaza and Bortolotti (1981). There are a series of NW-trending faults that truncate the Sierra de Velasco (Fig. 2), which have reactivated old early Paleozoic shear zones as defined by Höckenreiner et al. (2003). These NW-trending faults match the geometry and the distribution of the Tinogasta-Pituil-Antinaco (TIPA) shear zone system which generated a set of discrete mylonitic zones that coincides with the present NW structures (see Fig. 1 of Höckenreiner et al., 2003). Another alternative mechanism consistent with the source solutions is the active ENE-trending La Rioja fault system.

The Sierra de Ambato has a complex structure characterized by the N-trending Ambato fault which controls the western mountain front of this range (Fig. 2). The piedmont of the Sierra de Ambato between Andalgalá and Pomán in the north has a complex pattern of recent deformation affecting the alluvial cones and recent Quaternary deposits (Eremchuk, 1984). South of Pomán along the

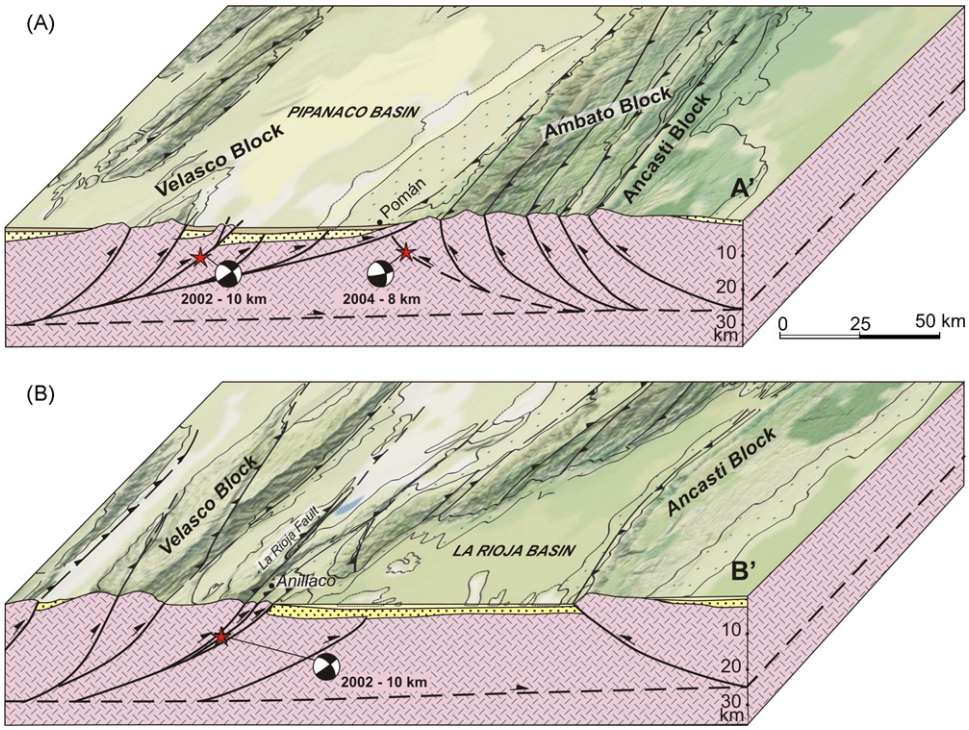

Fig. 4. Structural cross-sections of the study area. Constraints for the detachments have been obtained from deep seismic reflection studies of neighboring areas of Sierras Pampeanas and local focal mechanisms. Back hemispheres of the focal mechanism solutions are shown in vertical projection along the cross-section. See earthquake location and seismic source information in Fig. 2 and Table 1.

western border of Sierra de Ambato there is also evidence of prominent neotectonic activity (González Díaz, 1974). Pediments and alluvial fans are dissected by northeast-trending recent faults parallel to the main Ambato faults in the neighboring areas of the 1898 earthquake. Studies conducted in the Sierra de Ancasti (Fig. 2) also show Quaternary tectonic reactivation (Nullo, 1984), but not as significant as in the Ambato-Velasco zone.

A series of NNW oriented faults further to the east of the Ambato Fault imbricates the range, and its easternmost fault continues to the south matching the Ancasti Fault (Fig. 2). The Ancasti Fault seems to be the youngest structure of the eastern ranges since it truncates the imbricated faults of the Sierra de Ambato, such as is interpreted for similar out-of-sequence roof-thrust geometries of other regions (e.g. Butler, 2004; Holdsworth et al., 2006). All these main faults in the Sierras de Ambato and Ancasti are west vergent in contrast with the faults in the Sierra de Velasco, which have opposite vergence. It is interesting to analyze the central area where both systems get together. Surface structure shows that the east-vergent system is more active and is overimposed to the west verging faults. Details of the structure at depths have been constrained in other similar basement-cored uplifts of the southern Sierras Pampeanas using different scaled seismic methods, which involved focal mechanisms and deep seismic reflection data (Snyder et al., 1990). Cristallini et al. (2004) have presented an analogous structural model within the northern Sierras Pampeanas on the basis of high-quality deep seismic reflection profiles. Their findings are consistent with the interpretation of a basement wedge in the lower crust that is being transported to the east at depth. The structure at the surface, however, has opposite vergence mainly controlled by the fabrics and foliation of the metamorphic rocks (Ramos et al., 2002).

Studies of the La Rioja Basin east of the Sierra de Velasco using 2D seismic reflection data show that the reverse faults in the north are not continuous with those in the south and are separated by an accommodation east-trending zone intersecting La Rioja fault (Fig. 2). Thrust faulting in this framework can be accompanied by strike-slip structures, which passively displaces some subsurface faults in seismic reflection profiles (Fisher et al., 2002). It is worth to note that GPS data (Brooks et al., 2003) show that movement along the strike of the plate convergence decreases from north to south (Fig. 2), and there is no evidence for large strike-slip earthquakes. The northern block presents several small-offsets in ancient faults with a pre-Andean graben and half-graben geometry at the base of the basin of probable Cretaceous age. Superimposed is a Tertiary high angle thrust dipping less than 49° to the west, which is intersecting four sedimentary units, and is parallel to the exposed La Rioja thrust fault bounding the Sierra de Velasco in its eastern flank. The structure of the basin is related to the deformation front of the Sierra de Velasco and is probably a reactivated previous extensional fault according to Fisher et al. (2002). Its continuation at depths should be listric as commonly observed in other fault system geometries of the Sierras Pampeanas (Comíinguez and Ramos, 1991; Cristallini et al., 2004).

3.2. Tectonic regime and deep structure

Some authors have postulated an extensional mechanism for the formation of the Sierras Pampeanas (e.g. Fidalgo, 1963), a proposal that has been supported by analog modelling performed in laboratory in the 1980s. The opposite vergence between the Ambato block and the westernmost ranges led to Rossello and Le Corre (1989) to postulate the origin of this double vergence was a result of an extensional collapse. This extensional tectonic working hypothesis was used again by Gutiérrez (1999) and Mon (1999); in their view, the extension was the result of dominant strike-slip deformation in the Ambato block (see Fig. 1 in Gutiérrez, 1999) with an initial contraction in Late Miocene – Early Pliocene times and an extensional collapse in latest Pliocene Quaternary times (Mon, 1999). Further studies interpreted the present-day morphotectonic configuration of the Ambato block due to a Pleistocene left-lateral shear

zone along the major north–south Andean faults that bounded the Ambato block (Gutiérrez and Mon, 2008).

Although limited seismotectonic data are available, Fig. 2 shows that the majority of focal mechanisms in the region have reverse solutions and nodal planes consistent with the north-northeast strikes of major basement bounding active faults. The average *P*-axis orientation of the seismic focal mechanism estimations shows some obliquity with respect to the GPS velocity orientation in the region (~N76°E). On the other hand no major strike-slip components are observed in the northern sector of the area of study at the latitudes of the Ambato block, or in the southern sector corresponding to the Velasco region (Fig. 2).

Another feature derived from previous hypocenter determinations is their mid-to-lower crustal depths of 20–40 km (Figs. 2–4). These constraints provide insight on the deeper structural style of the Sierras Pampeanas. The structural cross-sections in Fig. 4 show a listric arrangement of faults at depth with an assumed décollement level between 25 and 28 km. Although there are no local constraints for these depths in the region, reprocessed deep seismic reflection studies in adjacent sectors of the Sierras Pampeanas are in agreement with this middle to lower crust estimation. Thus, in the Sierra de Valle Fértil and Sierra de La Huerta located between 30°S and 32°S, Snyder et al. (1990) obtained a décollement of less than 20-km depth composed of a series of west vergent thrusts. Further to the west along the boundary between Precordillera and Sierras Pampeanas at the Cerrito Salinas two décollement levels were recognized by Comíinguez and Ramos (1991). P-wave teleseismic receiver function analyses in that region of the Sierras Pampeanas around 30°S and 31.5°S also show the location of two intra-crustal arrivals which can be correlated with possible décollements that accommodated thrusting (Gilbert et al., 2006; Perarnau et al., in press). The lower level located at 27 km depth approximately for this region near 31.5°S, might be similar to the décollement depth assumed in the Ambato and Velasco cross-section area of Fig. 4.

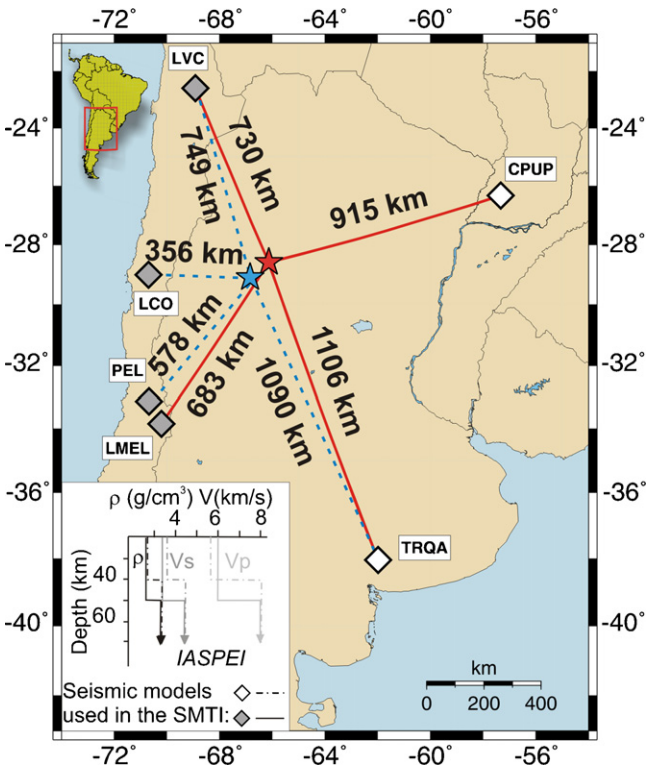

Fig. 5. Broadband seismic stations (Table 2) and epicentral distances used in the SMTI for the 2002 Velasco earthquake (shaded blue line) and the 2004 Ambato event (solid red line). Inset shows the P-wave velocity models used in the SMTI. Note that different crustal seismic velocity structures are used in the inversion of waveforms observed at stations CPUP and TRQA (eastern region mapping low elevation basement crust) and at stations LVC, LCO, PEL and LMEL (western region including the Andean Cordillera and Sierras Pampeanas). We used IASPEI model (Kennett and Engdahl, 1991) for the upper mantle seismic velocity structure. (For interpretation of the references to color in this figure legend, the reader is referred to the web version of the article.)

4. Seismic moment tensor inversion of the 2002 and 2004 crustal earthquakes

We have used a least square seismic moment tensor inversion (SMTI) technique in the time domain for a point source developed by Randall et al. (1995). It consists of modelling the complete three-component broadband seismograms at regional distances. The best solution corresponds to a minimum between predicted and observed waveform amplitudes and gives the seismic moment tensor for a fault plane dislocation. We assumed a seismic epicentral location from INPRES (Araujo et al., 2005) and performed a grid search for the hypocentral depth between 1 and 60 km with a grid spacing of 1 km. We obtained the best fit between predicted and observed waveforms and the seismic moment tensor for each depth. Thus we chose the best solution for the minimum amplitude misfit comparing the results for all trial focal depths. We also estimated the compensated linear vector dipole (CLVD) component which gives the non-double couple percentage component in the solution. We found the minimum amplitude misfit coincides with a CLVD component <20%.

The waveform modelling depends on a seismic velocity structure. This dependence increases with increasing wave frequency and decreasing epicentral distance. Broadband seismic stations operating in the region (Fig. 5 and Table 2) are very useful to study small-to-large earthquakes because it is possible to use waveforms that are not so distorted by the propagation effects and only depend on a regional seismic velocity structure. Seismic waves of periods longer than 10 s are less contaminated with noise than shorter-period data. For this reason, surface waves have been successfully used in the determination of seismic source parameters. Larger earthquakes generate sufficiently large surface waves at longer periods. In addition, using seismic velocity structures that map the differences between the western and eastern geologic terranes can

Table 2
Seismic stations used in the Seismic Moment Tensor Inversion of the 2002 and 2004 earthquakes.

Network	Station	Latitude (°S)	Longitude (°W)	Elevation (m)	Name	Region
IU-GE-GUC	LVC	22.6128	68.9113	2165	Limón Verde	Antofagasta, Chile
IU-DTM	LCO	29.0111	70.7010	2299	Las Campanas	La Serena, Chile
G-GUC	PEL	33.146	70.675	660	Peldehue	Santiago, Chile
IU-SJA	TRQA	38.0567	61.9795	501	Tornquist	Buenos Aires, Argentina
GT	CPUP	26.3306	57.3292	5	Villa Florida	Paraguay
GUC	LMEL	33.8476	70.2034	1540	Las Melosas	Refugio Las Melosas, Chile

IU = Global Seismograph Network (GSN-IRIS/USGS), GE = GEOFON Program, GFZ Potsdam, Germany, GUC = Departamento de Geofísica, Universidad de Chile, Chile, DTM = Carnegie Institution of Washington, G = Geoscope, SJA = Instituto Nacional de Prevención Sísmica (INPRES), San Juan, Argentina, GT = Global Telemetered Seismograph Network (USGS/USA).

produce better fits between synthetic and observed data (Alvarado et al., 2005a,b). Thus we combined a seismic model that takes into account the thicker crust of the Andean western terranes with higher P-wave velocity and P- to S-wave velocity ratio. For the raypaths travelling across the eastern basement and recorded at stations CPUP and TRQA (Table 2), the seismic model involves a thinner crust of smaller P-wave velocity and P- to S-wave velocity ratio (Fig. 4). We used the IASPEI upper mantle seismic velocity structure (Kennett and Engdahl, 1991) in both regions. We have also considered the curvature of the earth for making synthetic seismograms. This effect is particularly important for larger epicentral distances. We used "tkreflect" software which takes a spherical geometry with vertical variations of the seismic velocity structure parameters as input and converts it into an equivalent flat-layered earth model.

In the preparation of the data, we removed the instrument response from the observed waveforms and obtained the three-component seismic displacements. We rotated the north–south, east–west and vertical seismic displacements into vertical, radial and tangential orientations. We calculated Green's functions for the fundamental fault responses and marked the P-wave arrivals to align them with the observed data. This allows us to compare synthetic and observed data after the first arrival which minimizes location errors and dependence on the chosen seismic velocity structure. The last step before inversion was filtering the observed seismograms and Green's functions. We used a Butterworth bandpass filter testing for the lower and upper corner frequencies that permit to extract useful information based on data characteristics and high signal-to-noise quality. Waveforms of periods between 45 and 100 s gave good inversion results without excluding any component and thus warranting a good azimuthal coverage. This also prevented us from using weighting for the seismic components utilized during the inversion. However the distribution of the seismic stations ensures that closer stations, of relatively larger amplitudes and less noise, will have a major influence in the inversion. Nevertheless we tested the contribution of different combinations of station-components in the inversion to assess that they give similar inversion results.

4.1. The 28 May 2002 (M_w 5.8) Sierra de Velasco crustal earthquake

The earthquake on 28 May 2002 had its epicenter at approximately 35 km north of La Rioja in the eastern margin of the Sierra de Velasco (Araujo et al., 2005) (Figs. 1 and 2). La Rioja with an actual population of 150,000 inhabitants was seriously damaged in the past because of the occurrence of the 1894 earthquake, which had an epicentral location at about 180 km to the southwest from that city according to its seismic intensities (INPRES, 2010) (Fig. 1). Another earthquake in 1898 (Figs. 1 and 2) represents the most recent record of a moderate damaging event in the area. This previous seismicity, which affected regions which are now more densely populated, has been studied only qualitatively and categorized as moderate-to-large crustal seismic activity (INPRES, 2010). Comparatively, the 2002 event represents the first crustal earthquake of larger size in the region for which digital broadband seismic data are available. The event caused injury, severe damage and collapse of more than 100 houses in the epicentral area recording a maximum Modified Mercalli Intensity (MMI) of VIII in La Rioja (Araujo et al., 2005).

We computed the seismic moment tensor using broadband waveforms from four stations with epicentral distances between 356 and 1090 km (Fig. 5 and Table 2). We used a bandpass filter between 45 and 100 s. The minimum amplitude misfit (20%) between synthetic and observed waveforms occurs at a focal depth of 10 km with a CLVD component of 11% (Fig. 6). The SMTI results

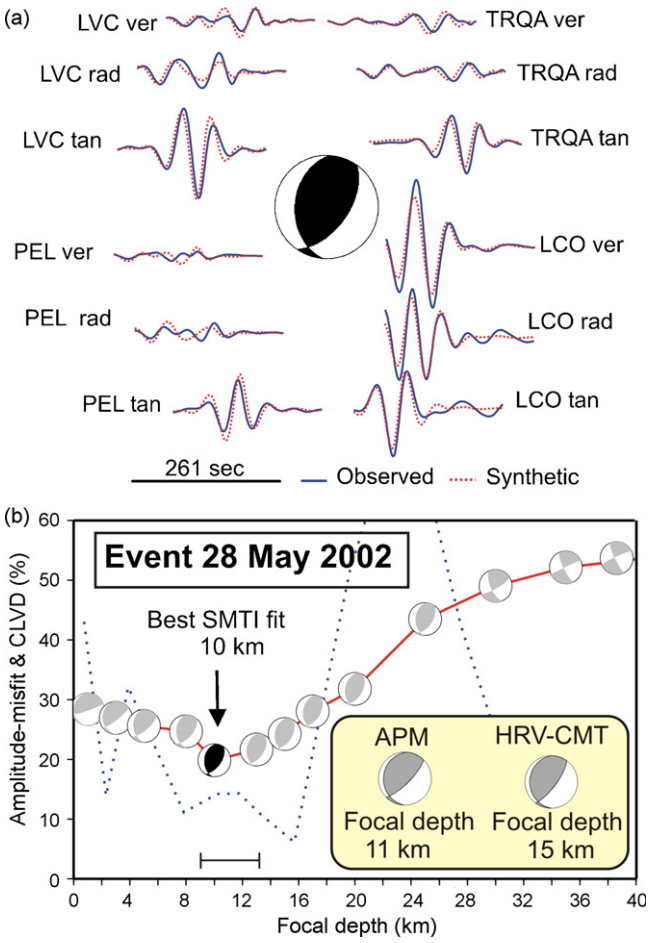

Fig. 6. SMTI results for the 28 May 2002 (Sierra de Velasco) earthquake. (a) Three component synthetic and observed broadband seismic displacements for the best depth (10 km) solution (see (b)) using the seismic stations shown in Fig. 5 and Table 2. (b) Amplitude-misfit error versus focal depth with lower hemisphere projection focal mechanisms obtained for each depth. For simplicity, results are shown only for a range of focal depths between 1 and 40 km, although inversions were performed at a series of fixed focal depths ranging from 1 to 60 km in steps of 1 km. Dotted-line is the CLVD component in each SMTI solution. The best fit between synthetic and observed waveforms (minimum amplitude-misfit error) occurs at a depth of 10 km. Focal depths between 9 and 13 km produce still acceptable fits. For comparison, previous determinations by Araujo et al. (2005) and Harvard-CMT (online catalogue) are shown with labels APM and HRV-CMT, respectively.

predict a focal mechanism of moment magnitude M_w 5.8 and seismic moment tensor of amplitude M_0 5.49×10^{17} Nm with fault plane solutions of approximately N–S strike (Table 1). Both fault plane solutions have a small strike-slip component. The focal mechanism solution is very stable for a widely tested focal-depth range although the best waveform-amplitude fits are found for a focal depth of 10 km. Including higher frequencies in our analysis would provide better resolution on the focal depth but require the implementation of a finer, more accurate, crustal velocity-depth model. This would be particularly necessary to study smaller events ($M < 5.0$). Although it is evident that different velocity-depth models represent the crust of the western versus eastern terranes of this region (see Fig. 5), a detailed knowledge of the velocity-depth crustal structure along the selected travel paths is not available. For this reason we preferred to use longer period waveforms, which are more insensitive to the chosen seismic velocity structure and give a range of acceptable waveform fits. However, we investigated the effects caused by different seismic models in the frequency range of data used for the SMTI analysis. We find that solutions with a misfit variation of +0.1 from the minimum estimate still

produce good fits between synthetic and observed data, which were calculated assuming hypocentral depths between 9 and 13 km (Fig. 6b).

Our SMTI solution is consistent with the P-wave first motion focal mechanism determined by Araujo et al. (2005) and their seismic location focal depth estimation. It is also in agreement with the Harvard CMT solution although the Harvard hypocentral depth was fixed (Table 1 and Figs. 3 and 6).

4.2. The 7 September 2004 (M_w 6.2) Sierra de Ambato crustal earthquake

The event on 7 September 2004 was located in the Sierra de Ambato at about 50 km in northeast direction from the 2002 earthquake epicenter in the Sierra de Velasco (Figs. 1 and 2). A maximum MMI of VIII was recorded in the epicentral area and of VI up to 50 km away from the 2004 epicenter. The event produced serious damage in several towns and historical sites (El Independiente, 2004; Catamarca al día, 2004; El Ancasti, 2004).

We have used high-quality regional broadband data from four stations in the region (Figs. 5 and Table 2) to estimate the seismic moment tensor of the 2004 earthquake. Preliminary results for this event indicated a thrust focal mechanism solution (Alvarado and Beck, 2005). We now used a more precise seismic location from Araujo et al. (2005) and broadband data filtered between 45 and 70 s to model full waveforms involving a sensitivity test of the source solution to variations in seismic velocity crustal models. Basically, two models consisting of one-layer over a halfspace were tested, which characterize the thicker crust of the Andean Cordillera and Sierras Pampeanas terranes in the west and the thinner crust of the more stable continental region in the east (inset in Fig. 5). Using the model proposed for the western terranes in the SMTI of the 2004 event (Western model curve in Fig. 7) significantly increases the amplitude misfit between synthetic and observed waveforms, with errors of more than 70% for the range of focal depths between 1 and 60 km. However, the double-couple focal mechanism and seismic moment tensor solution remain stable around the best depth using either velocity-depth structure. Overall the best SMTI solution was found for a seismic model that combines the different velocity-depth structures along each source-receiver travel path as shown in Fig. 5. The best solution corresponds to a thrust focal mechanism with a minimum amplitude misfit of 30% between synthetic and observed waveforms and a minimum (0%) in the CLVD component, a seismic magnitude M_w 6.2, a seismic moment M_0 2.23×10^{18} Nm, and a focal depth of 8 km (Fig. 7 and Table 1). Focal depths between 7 and 14 km are also acceptable.

As another way to test for the focal depth we have done a grid search using teleseismic depth-phase data. This technique is useful for estimating earthquake depth because the relative timing between the direct P-wave, and the free surface reflected pP and sP phases are linearly dependent on the focal depth parameter. In addition, relative amplitudes between these phases are linearly dependent on the seismic moment tensor and thus, can help to constrain the event mechanism (Spence et al., 1989; Goldstein and Dodge, 1999) (Fig. 8a). In practice, we assumed the SMTI focal mechanism solution (Fig. 7 and Table 1) and did a grid search around the focal depth to predict the relative polarities and timing of the P-wave depth phases at three teleseismic stations. These stations are located in the U.S.A. and Antarctica at epicentral distances between 36° and 78° from the 2004 epicenter (Fig. 8b). We concluded that assuming a focal mechanism with fault plane parameters: azimuth 32°, dip 74° and rake 90° (or azimuth 213°, dip 16° and rake 91°) the most reliable focal-depth estimation is 8 km, which predicts our depth phase identification in the observed vertical-component data. This is in agreement with the regional waveform modelling results.

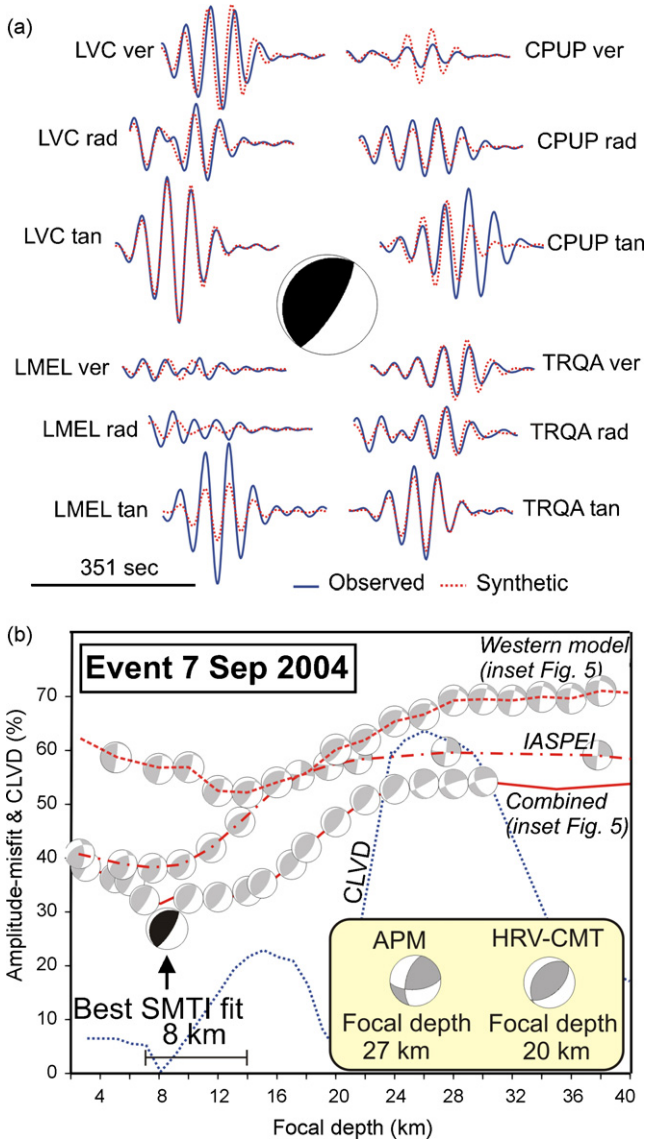

Fig. 7. SMTI results for the 7 September 2004 (Sierra de Ambato) earthquake. (a) Synthetic and observed broadband waveforms for the best depth (8 km) (see (b)) using the seismic stations shown in Fig. 5 and Table 2. (b) Amplitude-misfit error versus focal depth with lower hemisphere projection focal mechanisms obtained for each depth using the combined seismic velocity structure shown in inset of Fig. 5. Dotted-line is the CLVD component in each SMTI solution. Note the broader minimum around the selected depth (8 km); a range of acceptable focal depths is represented by the error bar. Also shown are the SMTI results using different seismic velocity structures for the western terranes (Fig. 5) and the IASPEI model (Kennett and Engdahl, 1991). Estimates by Araujo et al. (2005) and Harvard-CMT are plotted as APM and HRV-CMT, respectively.

The comparison of the SMTI solution with previous first motion and modelling determinations (Araujo et al., 2005 and Harvard-CMT catalogue) shows a dominant dip-slip component in the focal mechanism solution and a shallower focal depth for our constraint (Figs. 3, 7, 8 and Table 1). However *P*-axis orientations are similar (Table 1). The discrepancy with the hypocentral depth estimation by Araujo et al. (2005) might be expected since their estimation is based on seismic location methods, which is mainly affected by limitations of the earthquake location algorithms in determining accurately the focal depth parameter. On the other hand, the Harvard centroid moment tensor estimation for the focal depth is deeper than our SMTI solution but was fixed during their inversion (Fig. 3 and Table 1).

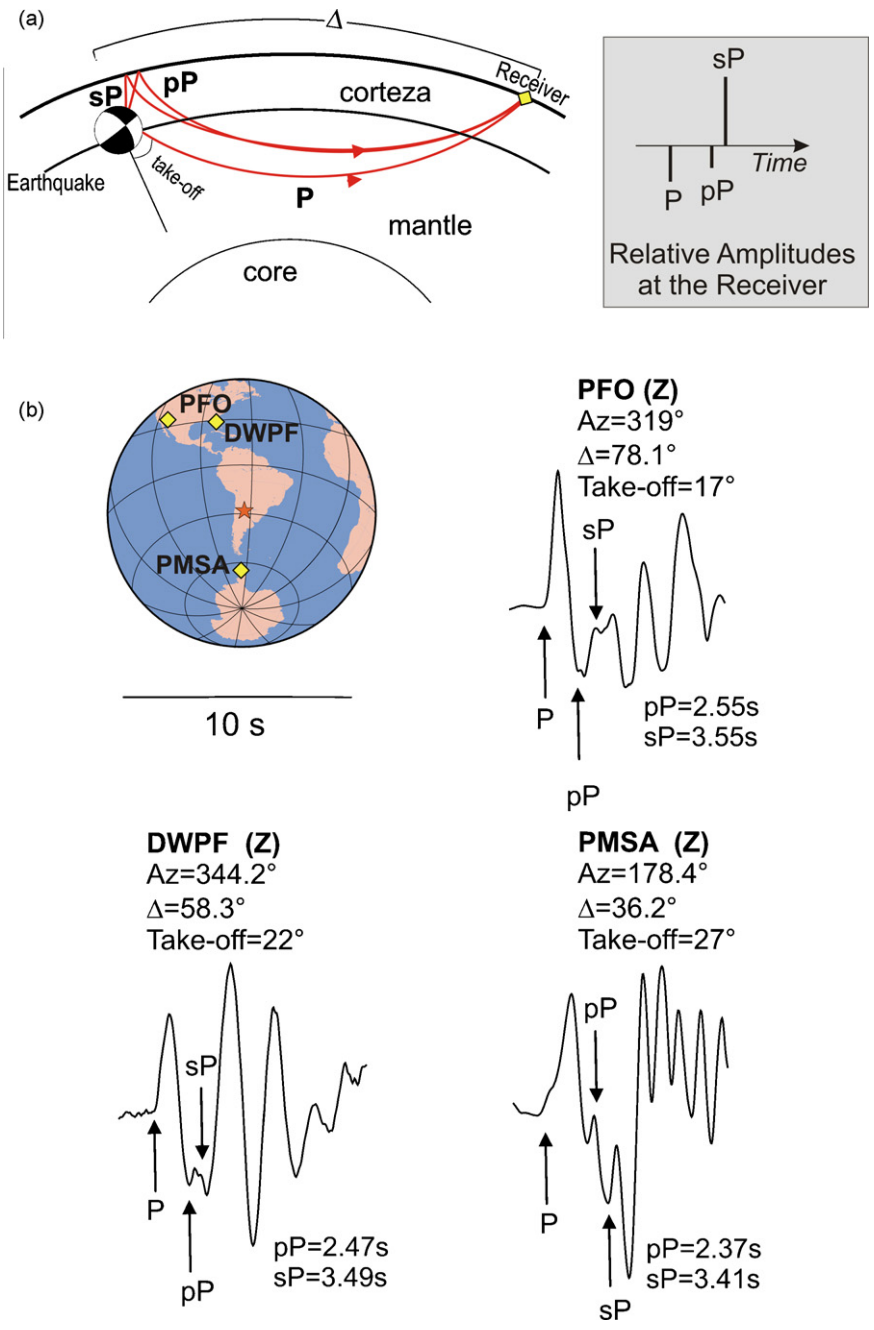

Fig. 8. (a) Ray path geometry and nomenclature of body-wave phases travelling from the source to the receiver for a simple model that comprises the crust and the mantle. Small P- and S-waves denote phases going up to the surface of the Earth, which are then reflected at this discontinuity before continuing their travel downward to the receiver as a P phase. (b) Comparison of body-wave phases using teleseismic broadband stations for the focal depth estimation of the 2004 Ambato earthquake. Arrows show predicted (downward and upward) depth phases at each station assuming the best focal mechanism solution and a focal depth of 8 km obtained from the SMTI analysis (Table 1 and Fig. 7). Delay times of the depth phases with respect to the direct P-wave arrivals at each station are also indicated.

5. Discussion

We have constrained the seismic moment tensor and focal depths for the most recent crustal earthquakes in 2002 and 2004 with location in the north western Sierras Pampeanas. Only eight seismic moment tensor determinations including our results for these two seismic events are available in this region (Table 1 and Fig. 2). Our SMTI used broadband data from four regional seismic stations which are part of global networks operating in the region and the Chilean seismic network. The results are based on the waveform matches between synthetic and observed complete seismic displacements. Besides the amplitude misfit we have included estimations of the CLVD component and tests of the effects of different crustal seismic models in the inversions to increase the reliability of our determinations. In order to improve the focal depth determinations we also performed teleseismic depth-phase analyses estimating a confidence interval on the focal depth of the larger 2004 earthquake.

Our SMTI results indicate moment magnitudes M_w 5.8 and 6.2 and hypocentral depths of 10 and 8 km for the 2002 and 2004 earthquakes, respectively. These estimations represent the larger seismic source sizes and shallower focal depths in the last 100 years in this region. We found predominately thrust focal mechanisms related to major double-couple force system solutions (CLVD

of 11% for the 2002 source solution and 0% for the 2004 event). We note that an association of these crustal earthquakes to individual faults is difficult because the subsurface geometry of the main structures in this region remains unknown. Scaling relationships predict small exposed ruptures (less than 10 km) for earthquakes of these moderate-to-high magnitudes (Wells and Coppersmith, 1994). These earthquakes, however, are consistent with previous focal mechanism determinations in this region and the orientations of active reverse faults, fractures and other zones of weakness in the Sierra de Ambato and Sierra de Velasco (Costa, 2008; Casa et al., 2009; in press).

This seismic region in the western Sierras Pampeanas is characterized by the emplacement of an orogenic belt with early Paleozoic magmatic rocks, which were heavily deformed during the Famatinian collision (Ramos, 1988, 2004; Astini et al., 1996). Significant shear zones were generated by that event as described by Höckenreiner et al. (2003) and Toselli et al. (2005). The main Andean faults coincide with mylonitic zones which clearly indicate that most of the Andean structures are controlled by pre-existing early Paleozoic fabrics. González Bonorino (1950) was the first to recognize that the main structural grain of the schistosity was controlling the inception and vergence of the faults. The western margin of the Sierra de Ambato coincides with a long-lived shear zone (González Bonorino, 1953), as well as the different faults observed in the Sierra de Velasco (Toselli et al., 1985; López et al., 1996; Höckenreiner et al., 2003). These pre-existing structures represent zones of weakness that seem to nucleate modern crustal seismicity as observed in other regions (Handy and Brun, 2004). As pointed out by Kirby (1985) and Sanchez et al. (2010) shear zones accommodate most of the strain in segments that are weaker than their surrounding rocks.

Seismic reflection and refraction data in the La Rioja basin indicate that reverse faults affect the highly reflective basement and cut sedimentary units of total thickness of about 3500 m in the east of Sierra de Velasco (Fisher et al., 2002) (Figs. 2 and 4). According to Fisher et al. (2002) younger reverse faults are located about 20 km east of the main Tertiary fault bounding the eastern margin of the Sierra de Velasco in the transition zone to the lower relief basement-involved block uplift of the Sierra Brava. Both reverse faults exhibit at the surface a high dip (<49°) angle to the west in their seismic line interpretation, which is a standard angle for a reverse fault produced by tectonic inversion of previous normal faults. The distribution of these reverse faults and their geometry are in agreement with reverse focal mechanism parameters for events AA-1979, AA-1983, AEA-2001 and the 2002 earthquake solution, which are consistent with a flattening at depth of any of these imbricated faults.

GPS observations in the study region are not dense. The two available measurements from Brooks et al. (2003) show the region is undergoing shortening along an approximate direction N75°E. Moment tensor summation over the larger crustal seismicity in the last 30 years shows an average *P*-axis horizontally oriented by an azimuth of 125° (plunge of 2°). The average *T*-axis is oriented by an azimuth of 241° and plunge of 58°. Our estimate for the maximum shortening orientation derived from the average *P*-axis orientation is clockwise rotated approximately 50° with respect to the plate tectonic convergence and GPS velocity vector orientations (Figs. 1 and 2). This suggests that ongoing thrusting earthquake deformation might be controlled by reactivated Paleozoic basement structures, which have a predominant northeast orientation in a zone of recurring seismic activity. This is also in agreement with neotectonic Quaternary observations from Costa (2008) and Casa et al. (in press), which indicate active deformation along probable inverted faults of mainly northeast strike.

The discrepancy in shortening orientations inferred from available GPS measurements and crustal earthquake focal mechanisms predicts some strike-slip motion along existing northeast oriented faults across this portion of the Sierras Pampeanas. However, there is no evidence for major strike-slip components in the earthquake source solutions. Perhaps this region includes some fault creeping behavior along N–S structures that do not build up the stress required to generate moderate-to-large strike-slip seismicity in this region. Another possibility could be the lower frequency of occurrence of strike-slip events having longer recurrence intervals in comparison with the more frequent thrusting earthquakes observed in the past 30 years. Eventually active strike-slip faulting along N–S trending structures could accommodate deformation further west in the forearc and intra-arc Andean regions although this type of seismicity has not been instrumentally recorded yet. Clear analogies to these alternative fault systems and seismicity exist in other seismic Andean segments (Cembrano et al., 2007; Lange et al., 2008; Alvarado et al., 2009b) and the Sumatran subduction zone (McCaffrey, 2009). In those margins, significant continental faults accommodate slip partition in the forearc region such as the forearc Liquiñe-Ofqui Andean Fault or the Sumatran Fault. We note that in any case, predominance of reverse focal mechanisms in the basement crust provides evidences for shortening and thickening of this sector of the Sierras Pampeanas in a very similar style of deformation to the Laramide models in western North America (e.g. Erslev, 1991; Narr and Suppe, 1994).

Interestingly, strain recorded by focal mechanisms of the larger seismicity in the last 30 years is very consistent with the vertical components of Quaternary neotectonic activity according to studies by Costa (2008) and Casa et al. (2009, in press). Dominant deformation in this part of the Sierras Pampeanas is mainly controlled by contraction which can be driven by regional compressional stresses as observed at present-day ruling out previous proposals, which suggested an extensional or sinistral regime for the geomorphic evolution since Pleistocene.

The occurrence of the 2004 earthquake in an adjacent segment of the 2002 event led us to think about the possibility that the former event might have triggered the second one as a consequence of a stress loading transfer (King et al., 1994). Our constraints can help to test this hypothesis but it is beyond the scope of this paper. From the seismic hazard point of view, the occurrence of the (Sierra de Velasco) 2002 earthquake in the epicentral area of the (Sierra de Ambato) 2004 earthquake may have worsened the effects of the later (2004) event in buildings and constructions inducing higher levels of seismic shaking intensities (the maximum MMI for the 2004 earthquake was of VIII according to Araujo et al., 2005).

In addition, we explored the crustal structure for the western and eastern terranes. Our SMTI results produced better seismogram fits using a thicker crust of 50 km thickness, P-seismic wave velocity (V_p) of 6.0 km/s and P-to-S seismic wave velocity ratio (V_p/V_s) of 1.80 for raypaths travelling from the 2004 hypocenter to the stations located in the west. The crust of the eastern terranes was best represented by a crustal model with a normal thickness of 40 km, V_p of 5.8 km/s and V_p/V_s of 1.68 (Figs. 5–7). These results are in agreement with estimations of crustal velocity-depth models over the flat-slab segment (Alvarado et al., 2005b).

6. Conclusions

We have used sparse broadband seismic stations from global networks and the Chilean national network to estimate the size, depth and focal mechanisms of two moderate crustal earthquakes in the northwestern Sierras Pampeanas in Argentina. The M_w 5.8 earthquake on 28 May 2002 with location in the eastern flank of the Sierra de Velasco and the M_w 6.2 event on 7 September 2004 with epicenter in the southwestern part of the Sierra de Ambato show shallow focal depths (10 and 8 km, respectively). These seismic events represent the larger seismicity in this region in a period of at least 100 years. The last earthquake of similar strength dates

back to 1898. We note that seismic activity concentrates in the fault system which connects Pampean ranges of opposite vergence, which runs from northeast (Ambato block) to southwest (Velasco block).

Focal mechanisms for larger crustal seismicity over the last 30 years reveals a similar deformation pattern as observed in neotectonic features since at least Pleistocene (Costa, 2008; Casa et al., 2009; in press), which is in agreement with a compressive regime where active faults are related to basement thrusts with very minor or inexistent strike-slip components. These facts rule out early proposals that claimed a combination of normal faults and strike-slip faults as the dominant mechanism of deformation in this sector of Sierras Pampeanas for the same time.

Historical seismicity and our determinations for the 2002 and 2004 earthquakes confirm that the reverse bounding faults of the Sierra de Velasco and Sierra de Ambato are still active and capable of generate moderate seismicity emphasizing the importance of inherited structural fabrics like faulting and shear zones in guiding intraplate deformation. The focal mechanism solutions for these events are providing evidence for competing styles of deformation in thrust-fault systems of opposite vergences. No major strike-slip components have been recorded for the larger seismicity instrumentally recorded. This evidence is in agreement with a backarc region in compression as observed by Pardo et al. (2002) and Alvarado et al. (2009a). Based on the geologic and seismic observations a regional extensional regime is very unlikely as the main mechanism of on-going deformation for the region, at least since the last 11,000 years. Extension is recorded by Mesozoic and older structures in the region though.

Although seismic location methods provide a first approximation of the focal depth which is useful in discriminating crustal events from slab events, seismic broadband modelling methods help to improve focal depth determinations. More refined focal depth estimations in the Andean foreland using high-quality broadband waveform data at regional distances and more appropriate crustal models (Alvarado et al., 2005a and this study) show discrepancies with global depth determinations which tend to be deeper. This is of importance in the assessment of the seismic hazard in this region; earthquakes of moderate-to-high (>6.0) magnitudes could produce serious damage based on their shallow focal depths. Examples of intraplate magnitude 6.3 earthquakes in other regions include the Bam, Iran event that occurred in December 2003 causing more than 30,000 deaths and the LÁquila, Italy earthquake that killed more than 250 people in March 2009.

Acknowledgments

We acknowledge the institutions referenced in Table 2 for providing us with broadband seismic data. Mauro Sáez helped us with the figures and seismic data preparation. We used the software SAC (Goldstein et al., 2003) to analyze seismic data and GMT to generate maps (Wessel and Smith, 1998). We thank the work of Chuck Ammon, Tom Owens and Philip Crotwell on seismic moment tensor inversion codes, seismic velocity models and corresponding documentation that we used. Financial support for this study came from the National Agency for Promotion of Science and Technology in Argentina (grants PICT2006-0122 and PICTO2007-0233) and the University of San Juan (CICITCA 2008-E814). This paper has been improved by valuable comments and suggestions of two anonymous reviewers and Dr. Carlos Costa.

References

Aceñolaza, F.G., Bortolotti, P., 1981. Estratigrafía y evolución tectónica de la Quebrada de La Rioja. 1st La Rioja Geology Symposium, Tucumán, Argentina. Acta Geológica Lilloana 15 (3), 31–39.

Alvarado, P., Beck, S., 2005. The Magnitude 6.2 Catamarca earthquake on 7 September 2004, Argentina. XVI Argentine Geological Congress, CD-ROM, Article 717, 8 pp.

Alvarado, P., Beck, S., 2006. Source characterization of the San Juan (Argentina) crustal earthquakes of 15 January 1944 (M_w 7.0) and 11 June 1952 (M_w 6.8). Earth and Planetary Science Letters 243, 615–631, doi:10.1016/j.epsl.2006.01.015.

Alvarado, P., Beck, S., Zandt, G., Araujo, M., Triep, E., 2005a. Crustal deformation in the south-central Andes back-arc terranes as viewed from regional broadband seismic waveform modelling. Geophysical Journal International 163, 580–598, doi:10.1111/j.1365-246X.2005.02759.x.

Alvarado, P., Castro de Machuca, B.M.E., Beck, S., 2005b. Comparative seismic and petrographic crustal study between the Western and Eastern Sierras Pampeanas region (31°S). Revista de la Asociación Geológica Argentina 60 (4), 787–796.

Alvarado, P., Pardo, M., Gilbert, H., Miranda, S., Anderson, M., Saez, M., Beck, S., 2009a. Flat-slab subduction and crustal models for the seismically active Sierras Pampeanas region of Argentina. Geological Society of America Memoirs 204, 261–278, doi:10.1130/2009.1204(12), Suzanne Kay, Victor Ramos, Williams Dickinson (Eds.), MWR204: Backbone of the Americas: Shallow Subduction, Plateau Uplift, and Ridge and Terrane Collision, Geological Society of America.

Alvarado, P., Barrientos, S., Saez, M., Astroza, M., Beck, S., 2009b. Source study and tectonic implications of the historic 1958 Las Melosas crustal earthquake, Chile, compared to earthquake damage. Physics of the Earth and Planetary Interiors 175, 26–36, doi:10.1016/j.pepi.2008.03.015.

Anderson, M., Alvarado, P., Zandt, G., Beck, S., 2007. Geometry and brittle deformation of the subducting Nazca plate, central Chile and Argentina. Geophysical Journal International 171 (1), 419–434.

Araujo, M.A., Pérez, A.M., Millán, M.H., 2005. The last destructive earthquakes occurred in La Rioja (05-28-2002) and Catamarca (09-07-2004), northwestern Pampean Ranges, Argentina. In: 6th International Symposium on Andean Geodynamic (ISAG, 2005), Extended Abstracts, Barcelona, Spain, pp. 53–56.

Arvidsson, R., Ekström, G., 1998. Global CMT analysis of moderate earthquakes, $M_w \geq 4.5$, using intermediate-period surface waves. Bulletin of the Seismological Society of America 88, 1003–1013.

Assumpção, M., 1992. The regional intraplate stress field in South America. Journal of Geophysical Research 97 (B8), 11889–11903.

Assumpção, M., Araujo, M., 1993. Effect of the Altiplano-Puna plateau, South America, on the regional intraplate stresses. Tectonophysics 221, 475–496.

Astini, R., Ramos, V.A., Benedetto, J.L., Vaccari, N.E., 1996. La Precordillera: un terreno exótico a Gondwana. XIII Congreso Geológico Argentino y III Congreso Exploración de Hidrocarburos, Buenos Aires. Actas V, 293–324.

Barazangi, M., Isacks, B., 1976. Spatial distribution of earthquakes and subduction of the Nazca plate beneath South America. Geology 4, 686–692.

Brooks, B.A., Bevis, M., Smalley, R., Kendrick, E., Manceda, R., Lauría, E., Maturana, R., Araujo, M., 2003. Crustal motion in the Southern Andes (26°–36°S): do the Andes behave like a microplate? Geochemistry Geophysics Geosystem 4 (1085), doi:10.1029/2003GC000505.

Butler, R.W.H., 2004. The nature of 'roof thrusts' in the Moine Thrust Belt, NW Scotland: implications for the structural evolution of thrust belts. Journal of the Geological Society 161 (5), 849–859.

Cahill, T., Isacks, B., 1992. Seismicity and shape of the subducted Nazca plate. Journal of Geophysical Research 97, 17503–17529.

Casa, A., Yamin, M., Cegarra, M., Coppolecchia, M., Costa, C., 2009. Deformación cuaternaria asociada al frente de levantamiento oriental de las Sierras de Velasco y Ambato. XIV Reunión de Tectónica de la Asociación Geológica Argentina, Río Cuarto, Córdoba, Argentina (abstract).

Casa, A.L., Yamin, M.G., Cegarra, M.I., Coppolecchia, M., Costa, C.H., in press. Deformación cuaternaria asociada al frente de levantamiento oriental de las Sierras de Velasco y Ambato. Revista de la Asociación Geológica Argentina.

Catamarca al día, 2004. Digital newspaper, Edition of September 24, 2004. Catamarca, Argentina.

Cembrano, J., Lavenu, A., Yañez, G., Riquelme, R., García, M., González, G., Hérail, G., 2007. Neotectonics. In: Moreno, T., Gibbons, W. (Eds.), The Geology of Chile. The Geological Society of London, pp. 231–261.

CERESIS, 2010. Centro Regional de Sismología para América del Sur, Intensidades sísmicas para los terremotos destructivos de Argentina, on-line catalogue (www.ceresis.org).

Chinn, D., Isacks, B., 1983. Accurate source depths and focal mechanisms of shallow earthquakes in western South America and in the New Hebrides Island arc. Tectonics 2 (6), 529–563, doi:10.1029/TC002i006p00529.

Comínguez, A.H., Ramos, V.A., 1991. La estructura profunda entre la Precordillera y Sierras Pampeanas (Argentina): evidencias de la sísmica de reflexión profunda. Revista Geológica de Chile 18 (1), 3–14.

Costa, C., 2008. Neotectónica. In: Peligrosidad sísmica en la Sierra de Velasco, SEGEMAR, Serie Contribuciones Técnicas Nro. 14, pp. 30–73. ISNN: 0328-9052.

Cristallini, E.O., Comínguez, A.H., Ramos, V.A., Mercerat, E.D., 2004. Basement double-wedge thrusting in the northern Sierras Pampeanas of Argentina (27°S); constraints from deep seismic reflection. In: McClay, K. (Ed.), Thrust Tectonics and Hydrocarbon Systems. AAPG Memoir 82, 65–90.

Dziewonski, A.M., Woodhouse, J.H., 1983. An experiment in systematic study of global seismicity; centroid-moment tensor solutions for 201 moderate and large earthquakes of 1981. Journal of Geophysical Research 88 (B4), 3247–3271.

Dziewonski, A.M., Chou, T.A., Woodhouse, J.H., 1981. Determination of earthquake source parameters from waveform data for studies of global and regional seismicity. Journal of Geophysical Research 86 (B4), 2825–2852.
El Ancasti, 2004. Digital newspaper, Edition of September 8, 2004.
El Independiente, 2004. Digital newspaper, Edition of September 8, 2004.
Eremchuk, J.E., 1984. Fracturas del borde occidental de las Sierras de Ambato-Manchao, provincia de Catamarca. 9th Argentinean Geological Congress, Bariloche, Argentina. Actas 2, 362–367.
Erslev, E.A., 1991. Trishear fault-propagation folding. Geology 19, 617–620.
Fidalgo, F., 1963. Algunos rasgos tectónicos y geomorfológicos de la Sierra de Sañogasta-Vilgo, provincia de La Rioja. Revista de la Asociación Geológica Argentina 18 (3–4), 139–153, Buenos Aires, Argentina.
Fisher, N.D., Jordan, T.E., Brown, L., 2002. The structural and stratigraphic evolution of the La Rioja basin, Argentina. Journal of South American Earth Sciences 15 (1), 141–156.
Gilbert, H., Beck, S., Zandt, G., 2006. Lithospheric and upper mantle structure of central Chile and Argentina. Geophysical Journal International 165, 383–398, doi:10.1111/j.1365-246X.2006.02867.x.
Goldstein, P., Dodge, D., 1999. Fast and accurate depth and source mechanism estimation using P-waveform modeling: a tool for special analysis, event screening, and regional calibration. Geophysical Research Letters 26 (16), 2569–2572.
Goldstein, P., Dodge, D., Firpo, M., Minner, L., 2003. SAC2000: signal processing and analysis tools for seismologists and engineers. In: Lee, W.H.K., Kanamori, H., Jennings, P.C., Kisslinger, C. (Eds.), Invited Contribution to The IASPEI International Handbook of Earthquake and Engineering Seismology. Academic Press, London.
González Bonorino, F., 1950. Algunos problemas geológicos de las Sierras Pampeanas. Revista de la Asociación Geológica Argentina 5 (3), 81–110, Buenos Aires, Argentina.
González Bonorino, F., 1953. Los supuestos depósitos de caolín en la falda occidental del Cordón Ambato (Catamarca). Revista de la Asociación Geológica Argentina 7 (3), 157–189, Buenos Aires, Argentina.
González Díaz, E.F., 1974. Superficies de erosión (abanicos rocosos) exhumadas en el flanco occidental de la Sierra de Ambato, al sur de la Quebrada de la Cebila (La Rioja), Argentina. Revista de la Asociación Geológica Argentina 29 (1), 5–22.
Gutiérrez, A.A., 1999. Tectonic geomorphology of the Ambato block (Northwestern Pampeanas Mountain Ranges, Argentina). In: 4th Andean Geodynamic Symposium, Göttingen, Germany, pp. 307–310.
Gutiérrez, A.A., Mon, R., 2008. Macroindicadores cinemáticos en el bloque Ambato, Provincias de Tucumán y Catamarca. Revista de la Asociación Geológica Argentina 63 (1), 24–28.
Gutscher, M.A., 2002. Andean subduction styles and their effect on thermal structure and interpolate coupling. Journal of South American Earth Sciences 15 (1), 3–10, doi:10.1016/S08959811(02)000020.
Gutscher, M., Spakman, W., Bijwaard, H., Enghdal, R., 2000. Geodynamics of flat subduction: Seismicity and tomographic constraints from the Andean margin. Tectonics 19, 814–833.
Guzmán, C., Cristallini, E., 2009. Contemporary stress orientations from borehole breakout analysis in the southernmost flat-slab boundary Andean retroarc (32°44′ and 33°40′S). Journal of Geophysical Research 114 (B02406), doi:10.1029/2007JB005505.
Guzmán, C., Cristallini, E., Bottesi, G., 2007. Contemporary stress orientations in the Andean retroarc between 34°S and 39°S from borehole breakout analysis. Tectonics 26 (TC3016), doi:10.1029/2006TC001958.
Handy, M.R., Brun, J.P., 2004. Seismicity, structure and strength of the continental lithosphere. Earth and Planetary Science Letters 223 (3–4), 427–441, doi:10.1016/j.epsl.2004.04.021.
Heidbach, O., Tingay, M., Barth, A., Reinecker, J., Kurfeß, D., Müller, B., 2008. The World Stress Map Database Release 2008 doi:10.1594/GFZ.WSM.Rel2008.
Höckenreiner, M., Söllner, F., Miller, H., 2003. Dating the TIPA shear zone: an Early Devonian terrane boundary between the Famatinian and Pampean systems (NW Argentina). Journal of South American Earth Sciences 16, 45–66.
Holdsworth, R.E., Strachan, R.A., Alsop, G.I., Grant, C.J., Wilson, R.W., 2006. Thrust sequences and the significance of low-angle, out-of-sequence faults in the northernmost Moine Nappe and Moine Thrust Zone. NW Scotland, Journal of the Geological Society 163 (5), 801–814, doi:10.1144/0016-76492005-076.
INPRES, 2010. Listado de terremotos históricos. On-line catalogue, www.inpres.gov.ar.
Introcaso, A., Lion, A., Ramos, V.A., 1987. La estructura profunda de las Sierras de Córdoba. Revista de la Asociación Geológica Argentina 42 (1–2), 177–187, Buenos Aires, Argentina.
Jordan, T.E., Allmendinger, R.W., 1986. The Sierras Pampeanas of Argentina: a modern analogue of Rocky Mountain foreland deformation. American Journal of Science 286, 737–764.
Jordan, T., Isacks, B., Ramos, V.A., Allmendinger, R.W., 1983a. Mountain building model: The Central Andes. Episodes 1983 (3), 20–26.
Jordan, T., Isacks, B., Allmendinger, R., Brewer, J., Ando, C., Ramos, V.A., 1983b. Andean tectonics related to geometry of subducted plates. Geological Society America Bulletin 94 (3), 341–361.
Kadinsky-Cade, K., 1985. Seismotectonic of the Chilean margin and the 1977 Caucete earthquake of western Argentina. Ph.D. Thesis, Cornell University, Ithaca, New York, USA, 253 pp.
Kay, S., Mpodozis, C., Ramos, V., Munizaga, F., 1991. Magma source variations for mid-late Tertiary magmatic rocks associated with a shallowing subduction zone and a thickening crust in the central Andes (28° to 33°S). In: Harmon, R.S., Rapela, C.W. (Eds.), Andean Magmatism and Its Tectonic Setting. Geol. Soc. Am. Spec. Pap. 265, Boulder, Co., USA, pp. 113–137.
Kendrick, E., Bevis, M., Smalley Jr., R., Brooks, B.A., Barriga, R., Lauría, E., Souto, L.P., 2003. The Nazca-South America Euler vector and its rate of change. Journal of South American Earth Sciences 16, 125–131.
Kennett, B.L.N., Engdahl, E.R., 1991. Traveltimes for global earthquake location and phase identification. Geophysical Journal International 122, 429–465.
King, G.C.P., Stein, R.S., Lin, J., 1994. Static stress changes and the triggering of earthquakes. Bulletin of the Seismological Society of America 84, 935–953.
Kirby, S.H., 1985. Rock mechanics observations pertinent to the rheology of the continental lithosphere and the localization of strain along shear zones. Tectonophysics 18, 1–27.
Lange, D., Cembrano, J., Rietbrok, A., Haberland, C., Dahm, T., Bataille, K., 2008. First seismic record for intra-arc strike-slip tectonics along the Liquiñe-Ofqui fault zone at the obliquely convergent plate margin of the southern Andes. Tectonophysics 455 (1–4), 14–24.
Langer, C.J., Bollinger, G.A., 1988. Aftershocks of the western Argentina (Caucete) earthquake of 23 November 1977: some tectonic implications. Tectonophysics 148, 131–146.
Langer, C.J., Hartzell, S., 1996. Rupture distribution of the 1977 western Argentina earthquake. Physics of the Earth and Planetary Interiors 94, 121–132.
Lithgow-Bertelloni, C., Guynn, J.H., 2004. Origin of the lithospheric stress field. Journal of Geophysical Research 109 (B01408.), doi:10.1029/2003JB002467.
López, J.P., Durand, F.R., Toselli, A.J., 1996. Zonas de cizalla en el flanco noroccidental de la Sierra de Velasco, La Rioja, Argentina. 13th Argentinean Geological Congress and 3rd Oil Exploration Congress, Buenos Aires, Argentina. Actas t. 2, 179–186.
Massabie, A., Limarino, C., Page, S., 1998. Estructura y actividad neotectónica en los Llanos de La Rioja, Sierras Pampeanas Noroccidentales, Argentina. 10th Latinamerican Congress. Actas v. II, 11–16.
McCaffrey, R., 2009. The tectonic framework of the Sumatran subduction zone. Annual Review of Earth and Planetary Sciences 37, 345–366, doi:10.1146/annurev.earth.031208.100212.
Mon, R., 1999. Normal faulting and major rock slides in the North Pampean Ranges of Argentina. In: 4th Andean Geodynamic Symposium, Göttingen, Germany, pp. 512–515.
Nábělek, J., 1984. Determination of earthquake source parameters from inversion of body waves. Ph.D. Thesis, Massachusetts Institute of Technology, Cambridge, Massachusetts, USA.
Narr, W., Suppe, J., 1994. Kinematics of basement-involved compressive structures. American Journal of Science 294, 802–860.
Nullo, F.E., 1984. Estructura del extremo austral de la Sierra de Ancasti, Catamarca. 9th Argentinean Geological Congress, Bariloche, Argentina. Actas 2, 414–426.
Pardo, M., Comte, D., Monfret, T., 2002. Seismotectonic and stress distribution in the central Chile subduction zone. Journal of South American Earth Sciences 15 (1), 11–22.
Perarnau, M., Alvarado, P., Saez, M., in press. Estimación de la estructura cortical de velocidades sísmicas en el suroeste de la Sierra de Pie de Palo, provincia de San Juan (Argentina). Revista de la Asociación Geológica Argentina.
Ramos, V.A., 1988. Tectonics of the Late Proterozoic – Early Paleozoic: a collisional history of Southern South America. Episodes 11 (3), 168–174.
Ramos, V.A., 1999. Plate tectonic setting of the Andean Cordillera. Episodes 22 (3), 183–190.
Ramos, V.A., 2004. Cuyania, an exotic block to Gondwana: review of a historical success and the present problems. Gondwana Research 7 (4), 1009–1026.
Ramos, V.A., Cristallini, E.O., Pérez, D.J., 2002. The Pampean flat-slab of the central Andes. Journal of South American Earth Sciences 15, 59–78.
Randall, G.E., Ammon, C.J., Owens, T.J., 1995. Moment-tensor estimation using regional seismograms from a Tibetan Plateau portable network deployment. Geophysical Research Letters 22, 1665–1668.
Rossello, E.A., Le Corre, C., 1989. Los bloques basculados de las Sierras de Ambato y Ancasti (Catamarca, Argentina): responden a un modelo neógeno de fallamiento lístrico distensivo o compresivo? Primera Reunión de Fallas Activas del Noroeste Argentino. GETEC. Universidad Nacional de San Juan (San Juan, Argentina), Actas.
Sanchez, G., Rolland, Y., Schreiber, D., Giannerini, G., Corsini, M., Lardeaux, J.M., 2010. The active fault system of SW Alps. Journal of Geodynamics 49 (5), 296–302.
Smalley Jr., R., Pujol, J., Regnier, M., Chiu, J.M., Chatelain, J.L., Isacks, B.L., Araujo, M., Puebla, N., 1993. Basement seismicity beneath the Andean Precordillera thin-skinned thrust belt and implications for crustal and lithospheric behavior. Tectonics 12, 63–76.
Snyder, D.B., Ramos, V.A., Allmendinger, R.W., 1990. Thick-skinned deformation observed on deep seismic reflection profiles in Western Argentina. Tectonics 9 (4), 773–788.
Spence, W., Sipkin, S.A., Choy, G.L., 1989. Measuring the size of an earthquake. Earthquakes and Volcanoes 21 (1), 58–63.
Toselli, A.J., Rossi, J., Aceñolaza, F., 1985. Milonitas de bajo grado de la megafractura de Sierras Pampeanas en la Quebrada de La Rioja, Sierra de Velasco, Argentina. 4th Congreso Geológico Chileno. Antofagasta, Antofagasta, Chile. Actas T.1 Area 2, 160.
Toselli, A.J., Aceñolaza, F.G., Bossi, J.N., 2005. Esquema geológico de la Sierra de Velasco, Argentina. 16° Congreso Geológico Argentino, Actas 1, 129–132.
Triep, E.G., 1979. Source mechanism of San Juan Province earthquake, 1977. International Institute of Seismology and Earthquake Engineering (Japan), Individual Studies 15, pp. 1–14.

Vigny, C., Rudloff, A., Ruegg, J.C., Madariaga, R., Campos, J., Alvarez, M., 2009. Upper plate deformation measured by GPS in the Coquimbo gap, Chile. Physics of the Earth and Planetary Interiors 175 (1–2), 86–95.

Wells, D.L., Coppersmith, K.J., 1994. New empirical relationships among magnitude, rupture length, rupture width, rupture area, and surface displacement. Bulletin of the Seismological Society of America 84, 974–1002.

Wessel, P., Smith, W.H.F., 1998. New, improved version of generic mapping tools released, EOS. AGU 579.

WSM-Project, 2010. The World Stress Map Project – A Service for Earth System Management. German Research Centre for Geosciences-GFZ Helmholtz Centre Potsdam, Germany, Available from: http://dc-app3-14.gfz-potsdam.de/.